

Mach Zender Interferometer: Design of Experiment Proposal

Clary, Matt
matthewcclary@gmail.com
Username: matthewcclary

Index Terms—Silicon Photonics, Mach Zender Interferometer, Design of Experiment

1 INTRODUCTION

To accurately design and predict the behavior of complex photonic circuits, a precise understanding of waveguide properties is essential. Among these properties, the **group index** (n_g) is a critical parameter that determines the speed at which information travels through the waveguide and governs the wavelength-dependent behavior of many devices, including filters, modulators, and sensors.

This project proposes the design and fabrication of an interferometer device to experimentally determine the group index of silicon waveguides.

The design objectives include:

- Develop a reliable experimental method for measuring group index in silicon waveguides
- Validate theoretical models against experimental data
- Characterize the impact of waveguide geometry on group index
- Establish a systematic approach for group index measurement in integrated photonic devices

The proposed design will utilize a **Mach-Zehnder Interferometer (MZI)** to create a periodic optical response, from which the group index can be directly extracted. The **FSR (Free Spectral Range)**, determined by the group index and the length difference between the MZI arms, will be designed to be measurable within the available experimental bandwidth.

2 THEORY

The group index is defined as the ratio of the speed of light to the group velocity of light in the waveguide.

The group index is given by:

$$n_g = n_{eff} - \lambda \frac{dn_{eff}}{d\lambda} \quad (1)$$

where n_{eff} is the effective index and λ is the wavelength.

For an imbalanced Mach-Zehnder Interferometer, the transfer function is given by:

$$\frac{I_o}{I_i} = \frac{1}{2} \left[1 + \cos \left(\frac{2\pi n_g \Delta L}{\lambda} \right) \right] \quad (2)$$

where ΔL is the length difference between the MZI arms.

The FSR is related to the group index by:

$$FSR = \frac{\lambda^2}{n_g \cdot \Delta L} \quad (3)$$

This relationship allows direct extraction of the group index from FSR measurements.

3 MODELLING AND SIMULATION

3.1 Waveguide Design

For the main DOE, a **500nm wide by 220nm thick strip waveguide** will be used. This waveguide consists of a silicon core in a silicon dioxide cladding.

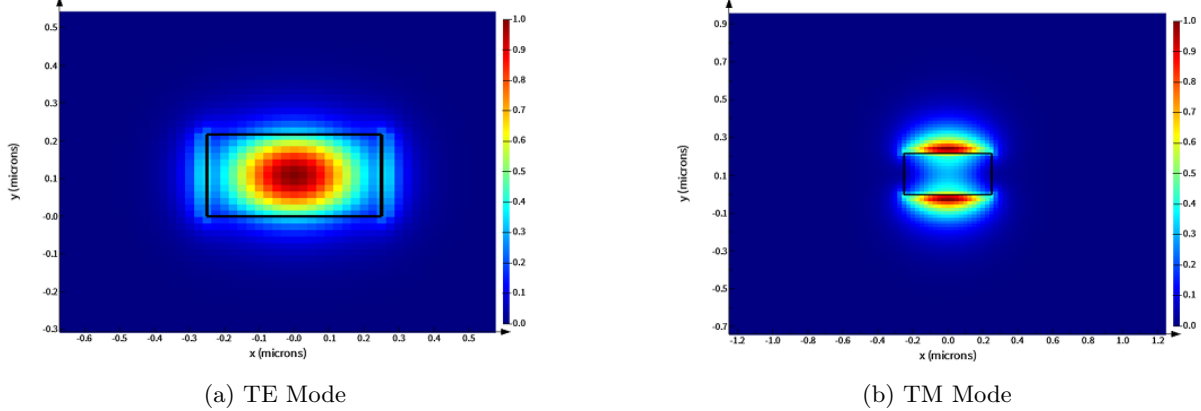


Figure 1: Silicon waveguide mode profiles showing (a) TE mode and (b) TM mode field distributions.

The compact model for the effective index of the silicon waveguide is given by:

$$n_{eff}(\lambda) = 2.44 - 1.13(\lambda - 1.55) - 0.044(\lambda - 1.55)^2 \quad (4)$$

where λ is the wavelength in micrometers.

The effective index and group index versus wavelength for the silicon waveguide are shown in Figure 2.

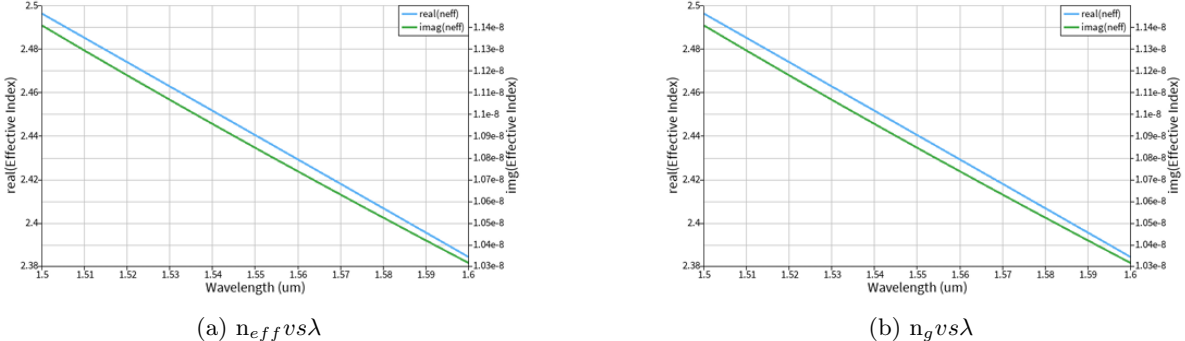


Figure 2: Effective index and group index versus wavelength for the silicon waveguide.

3.2 MZI Circuit Design

The MZI circuit will be designed with a y-branch splitter connected to 2 waveguides. One of the waveguides will remain constant in length at $50\mu\text{m}$, while the other one will vary to create our ΔL . These waveguides will then be brought back together with a y-branch combiner. Both y-branches will terminate at a grating coupler for measurement.

The transmission spectrum for this circuit can be seen in Figure 4.

3.3 Parameter Variation Analysis

The ΔL values that will be implemented in the DOEs are shown in Table I.

A value of $30\mu\text{m}$ was chosen to achieve an FSR close to the maximum allowed by the measurement setup. The goal was then to cover a wide range to create a clearer trend of the FSR decreasing with increasing ΔL . The plan is also to include multiple splits of the $200\mu\text{m}$ ΔL to observe the process

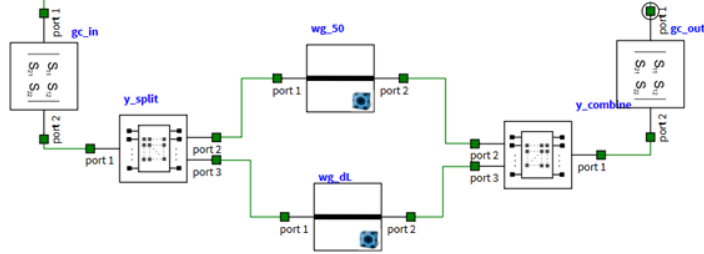


Figure 3: High-level schematic of the MZI circuit design showing y-branch splitters, variable arm lengths, and grating couplers.

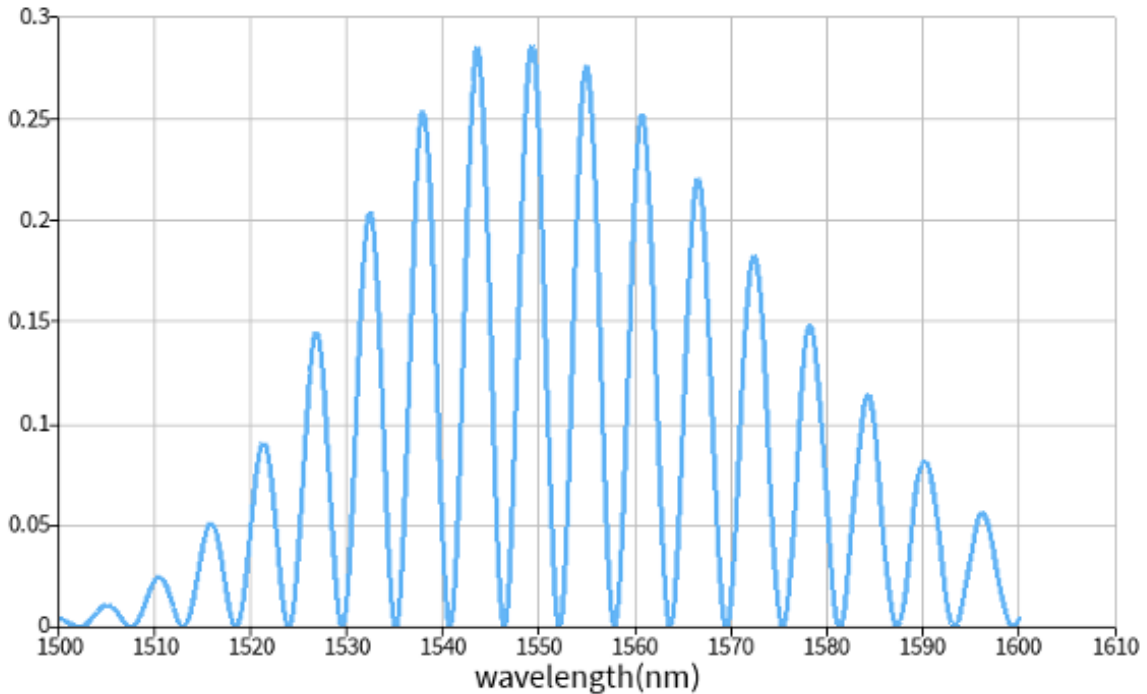


Figure 4: Transmission spectrum for MZI with $\Delta L = 100 \mu\text{m}$ showing periodic FSR response.

variation effects on FSR. With such a small FSR, variations in the process will be more apparent in the results. If space allows, the plan would be to explore adding an MZI or two that use a slightly wider waveguide.

4 FABRICATION

The Mach-Zehnder Interferometer (MZI) devices will be fabricated on a standard Silicon-on-Insulator (SOI) platform with a 220 nm silicon device layer and a 3 μm buried oxide (BOX) layer. The patterning of the strip waveguides, couplers, and grating structures will be achieved using high-resolution Electron Beam Lithography (EBL), followed by a dry etch process to define the silicon structures. The sample will then be passivated with an SiO_2 overcladding layer to provide thermal stability and protection. The layout I fabricated consists of both TE and TM test structures, as well as 2 calibration structures to help clean up the spectrum for our analysis. The complete device layout, including the various ΔL designs, along with 2 calibration structures, and the input/output grating couplers, is shown in Figure 5.

Table 1: MZI ARM LENGTH DIFFERENCE AND RESULTING FSR

ΔL (μm)	FSR (nm)
30	19.19
50	11.4
100	5.7
150	3.8
200	2.8

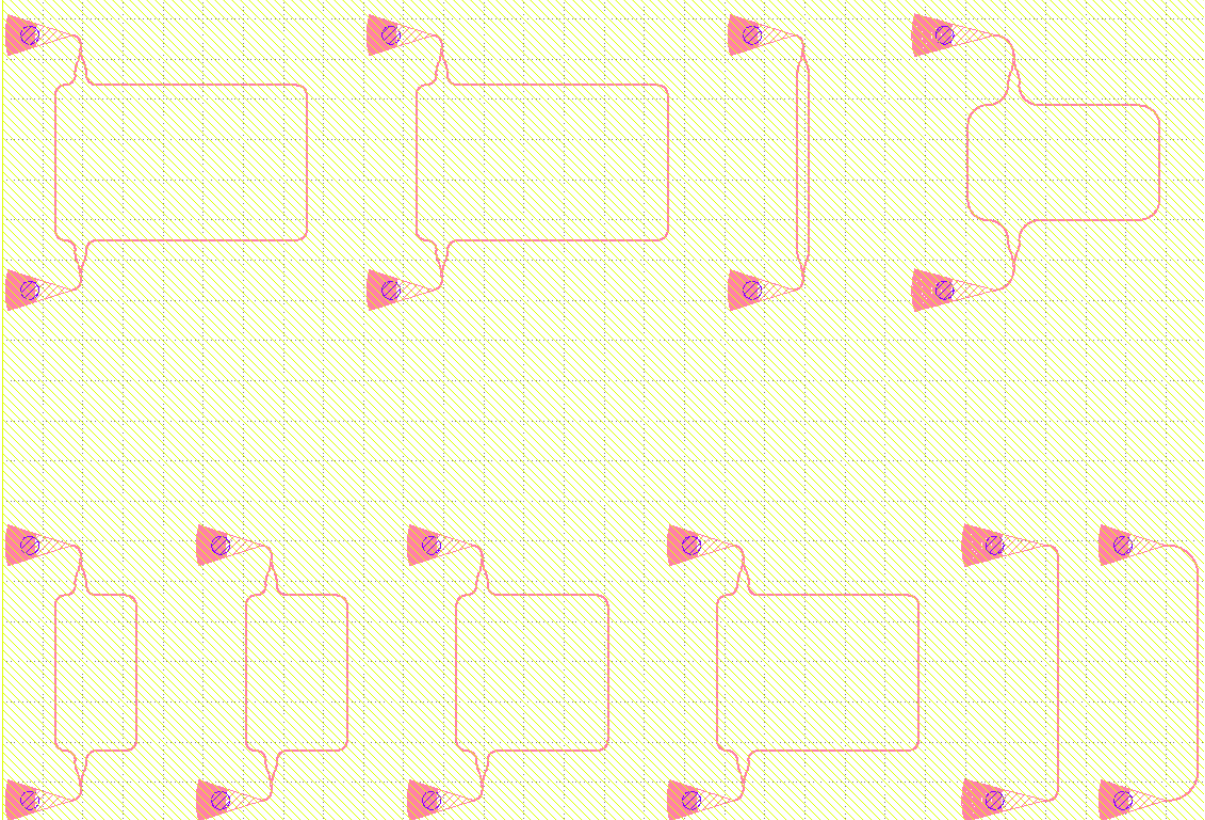


Figure 5: Full device layout showing the placement of the MZI structures with varying ΔL , along with the input and output grating couplers.

5 EXPERIMENT DATA

The fabricated Mach-Zehnder Interferometers (MZIs) were characterized using a tunable laser and a power meter. The transmission spectra were measured across the C-band (1530 nm to 1565 nm) for all varying path length differences (ΔL). All devices were tested under the same optical power and coupling conditions.

The analysis focuses on extracting the Free Spectral Range (FSR) from the measured data to determine the group index (n_g), as established in Equation (3).

Figure 6 presents the measured transmission spectra for the $\Delta L = 100 \mu\text{m}$ device, comparing the fundamental **TE** and **TM** polarizations. The TE mode shows clearly defined, high-visibility fringes (Figure 6a), while the TM mode exhibits a different FSR, confirming the birefringence of the waveguide (Figure 6b).

To assess the impact of process variation, two distinct $\Delta L = 200 \mu\text{m}$ TE test structures were measured. As anticipated by the simulation (Table I), these devices exhibit a much smaller FSR, making them sensitive to minor fabrication inconsistencies. Figure 7 shows the comparison between the two structures, with subtle differences in FSR and fringe visibility indicating localized process variations (Figures 7a and 7b).

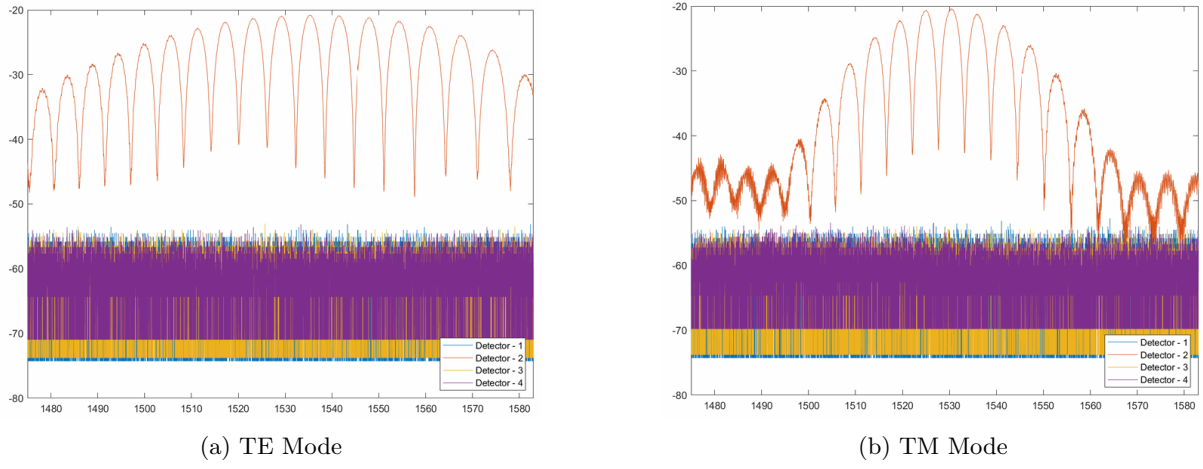


Figure 6: Transmission spectra for the $\Delta L = 100 \mu\text{m}$ MZI, comparing TE and TM polarization measurements.

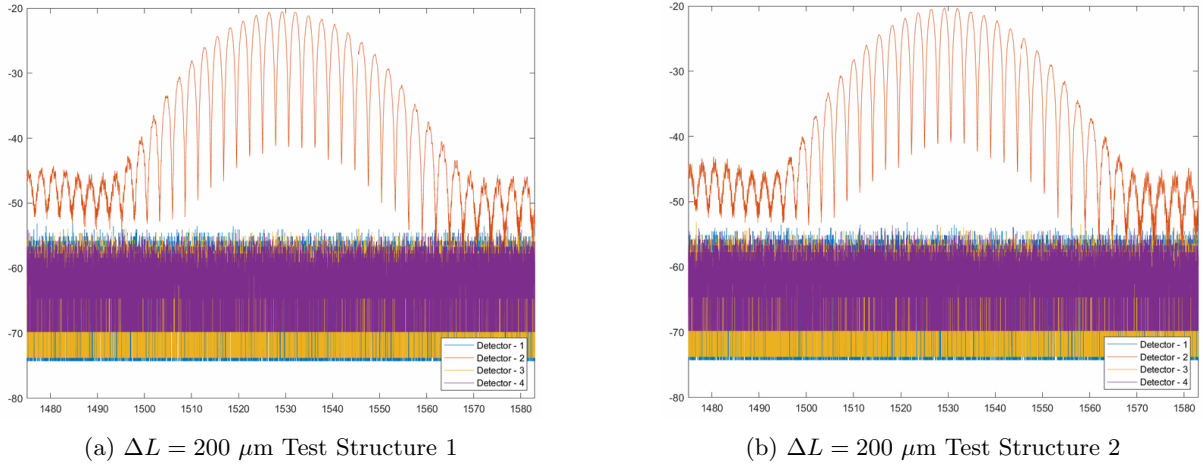


Figure 7: Transmission spectra comparing two $\Delta L = 200 \mu\text{m}$ TE test structures. Subtle differences in FSR highlight process variations.

6 ANALYSIS

In an incredibly unfortunate turn of events, my computer's harddrive locked out and I lost everything associated with this course (that wasn't submitted online). I tried to re-access the data and reinstall software but exhausted all possible solutions. As such, all I have is the experimental results and the initial work that went into the first report. All of my corner analysis work was also lost.

7 CONCLUSION

My conclusions are limited as I could not complete the final comparison of the measured circuits to my simulations. I did learn a lot from the corner analysis work that I was able to do before losing everything and found the process of correlating the results fascinating and look forward to applying it in my professional work.

ACKNOWLEDGMENTS

I would like to thank Prof. Chrostowski for putting this course together and the guidance in reaching this point. As well as for access to the tools and facilities to make this project a reality. Also to the rest of the team for making themselves available to answer questions and troubleshoot issues.